# Mixed-Surfactant-Induced Morphology Change of Polyaniline

**Chia-Fu Chen,[1] I-Ann Lei,[1] Wen-Yen Chiu[1,2,3]**

[1]*Department of Chemical Engineering, National Taiwan University, Taipei, Taiwan*
[2]*Department of Material Science and Engineering, National Taiwan University, Taipei, Taiwan*
[3]*Institute of Polymer Science and Engineering, National Taiwan University, Taipei, Taiwan*

Received 21 March 2010; accepted 10 October 2011
DOI 10.1002/app.36393
Published online in Wiley Online Library (wileyonlinelibrary.com).

**ABSTRACT:** In this study, polyaniline (PANI) was synthesized in the presence of a mixture of two surfactants, dodecylbenzene sulfonic acid (DBSA) and sodium dodecyl sulfate (SDS). The morphology of PANI observed under transmission electron microscopy was found to be spherical and cylindrical shapes. At low DBSA concentrations (2 and 10 m*M*), the addition of SDS made it easier to obtain the cylindrical morphology of PANI. A scheme based on the deformation and coagulation of mixed micelles was proposed to explain the morphological change of PANI. In the system of 10 m*M* DBSA, when the SDS concentration was 2 m*M*, the tubular morphology of PANI was observed, whereas when the SDS concentration was increased, a fiber morphology of PANI was found. The relative ratio of anilinium cations to free aniline played a key role in whether the tube or fiber morphology existed. Finally, a significant improvement in the conductivity of PANI was achieved when PANI had a cylindrical morphology. © 2012 Wiley Periodicals, Inc. J Appl Polym Sci 000: 000–000, 2012

**Key words:** conducting polymers; morphology; surfactants

## INTRODUCTION

Conducting polymers, including polypyrrole, polythiophene, and polyaniline (PANI), are potentially useful in many applications, including electromagnetic shielding, conducting paints, and electronic devices. Among these polymers, PANI has very high environmental stability and is easy to prepare with low costs. PANI is usually synthesized by the oxidative polymerization of aniline in an acid medium with the addition of ammonium peroxydisulfate (APS) as the oxidant.[1,2] Its conductivity has been found to depend very much on its oxidation state, and its emeraldine salt is most electrically conductive and can be doped from emeraldine base with protonic acid. However, the main problem of PANI related to potential applications is its processability. Some reports have shown that the production of colloidal PANI could improve its processability.[3–7] Vincent and Waterson[3] prepared spherical and needle-type PANI by using different copolymers as the steric stabilizers. Yu el al.[6] synthesized particulate and fiberlike PANI through various concentrations of aniline, HCl, and sodium dodecyl sulfate (SDS). By changing the concentrations of aniline and SDS, one can change the morphology of dispersed PANI to fiberlike or coil-like. This is mainly due to a change of micellar structure with increasing SDS concentration.

Other methods for preparing PANI, including the emulsion polymerization process,[8–11] polymerization of aniline in micelles,[12,13] and reversed microemulsion,[14] have been reported. An alternative way to prepare colloidal conducting polymers involves the coating of latex particles with a thin layer of conjugated polymers to form conductive composites with a core–shell morphology; these include PANI-coated polystyrene and polypyrrole-coated poly(butyl methacrylate).[15] The core–shell morphology[16–18] effectively improves the processability and demonstrates high conductivity with low conducting polymer loading. Another way to improve the processability of PANI is to synthesize a PANI–poly(4-styrenesulfonic acid) composite by polymerization of aniline in the presence of poly(4-styrenesulfonic acid).[19–21]

Furthermore, to obtain a high conductivity of PANI, the choice of dopants is very important. Several dopants have been used, including as camphor sulfonic acid, hydrochloric acid, and dodecylbenzene sulfonic acid (DBSA).[22,23] Kuramoto and Genies[22] reported that the concentration of the DBSA dopant more significantly influenced the conductivity of PANI than that of the HCl dopant.

In a previous study, we found that with different added concentrations of SDS, HCl, and DBSA, the morphology of PANI on polyurethane/PANI core–shell particles could vary from spherical to

*Correspondence to:* W.-Y. Chiu (ycchiu@ntu.edu.tw).

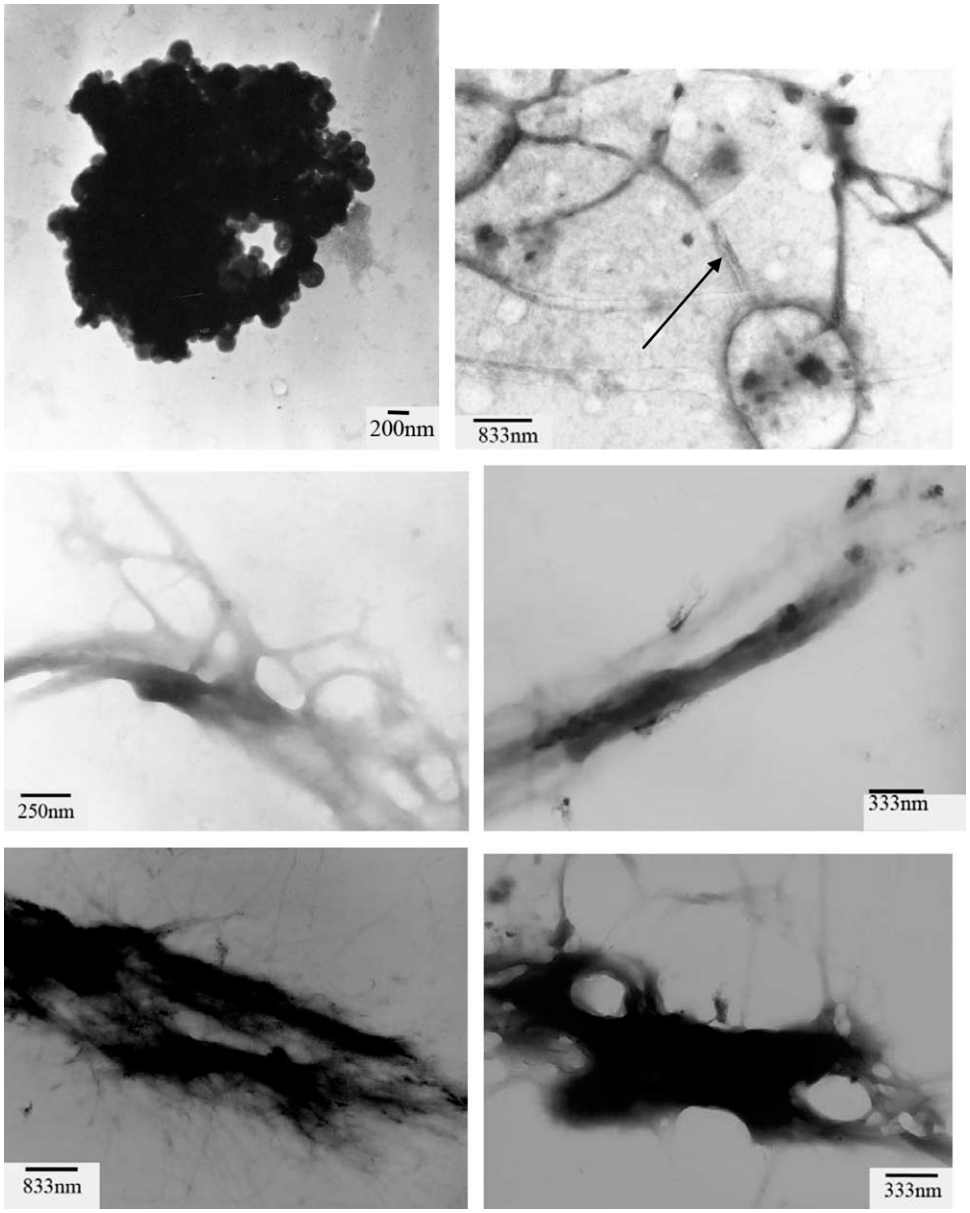


**Figure 1** TEM photographs of PANI with DBSA fixed at 10 m*M* and SDS: (a) 1 m*M* PANID02S01, (b) 2 m*M* PANID02S02, (c) 3 m*M* PANID02S03, (d) 5 m*M* PANID02S05, (e) 7 m*M* PANID02S07, and (f) 10 m*M* PANID02S10.

cylindrical.[24] In this research, we focused on the morphological change of synthesized PANI in the presence of a mixture of surfactants. The concentrations of DBSA and SDS were varied to induce different morphologies in PANI. The Fourier transform infrared (FTIR) spectra, ultraviolet–visible (UV–vis) spectra, and conductivities of the product samples were examined and are discussed.

## EXPERIMENTAL

### Materials

Aniline, DBSA, SDS, APS, hydrochloric acid, and sodium chloride were purchased from Acros (Geel, Belgium) and were used as received.

### Preparation of PANI

DBSA and SDS were dissolved separately in deionized water, and aniline was added after the DBSA and SDS solutions were mixed. The concentration of aniline was 10 m*M* for each sample. APS was used as an oxidant, and an equal molar concentration of APS with respect to the aniline monomer was used for each sample. The reaction was carried out under vigorous stirring at room temperature for 24 h. The collected latex was centrifuged several times with methanol and water before being dried in a vacuum oven at 110°C.

### Characterization

The morphology of the latex was examined by transmission electron microscopy (TEM; Hitachi, Tokyo,

Japan, H-7100). The samples were diluted to have a solid content of 1 wt %. Samples were placed on grids and dried at room temperature before the TEM experiments were performed.

The UV–vis spectra of the latex emulsions were measured by UV–vis spectrometry (HEλIOS γ, Omaha, NE, USA). The latex emulsions were diluted and placed in a quartz cell before the UV–vis scans were performed.

The FTIR spectra were measured by a Bio-Rad (Hercules, CA, USA) FTS 3000 instrument. The latex was centrifuged several times with distilled water and methanol before being dried to obtain dry samples. The dry samples were then mixed with KBr before they were pressed into pellets. Each pellet was scanned, and 64 scans were obtained.

The particle size distribution was investigated by dynamic light scattering (DLS; Zetasizer Nano-ZS, Malvern, UK).

The X-ray diffraction (XRD) studies were performed with MAC Science (Tokyo, Japan) Diffractometer MXP-3.

The conductivities of PANI were measured with standard four-probe technology in the form of pellets. The thickness of the films was determined with a Digimatic micrometer APB-2D from Mitutoyo (Kanagawa, Japan). Then, the electrical conductivity of the films (ρ) was determined from eq. (1):

$$\rho = \frac{t}{RA} \tag{1}$$

where $t$ is the thickness of film, $R$ is the surface electrical resistance, and $A$ is the cross-sectional area of film.

The surface tension of the surfactant solution was measured by a SINTERFACE (Berlin, Germany) tensiometer PAT-2P. Each sample was stirred for 30 min before undergoing surface tension measurement. The obtained surface tension for each sample was an average of 15 subruns.

## RESULTS AND DISCUSSION

The TEM photographs of the PANI latex are shown in Figures 1–3. Figure 1(a–f) shows the morphology of PANI when the concentration of DBSA was 10 m*M*. As shown in Figure 1(a), when SDS was 1 m*M*, the morphology of PANI was mainly spherical with severe aggregation. When concentration of SDS increased to 2 m*M*, as indicated by an arrow in Figure 1(b), PANI with a tubular morphology was observed. When SDS was increased more to 3 or 10 m*M*, as shown in Figure 1(c–f), PANI with a fiber morphology was found. For a concentration of DBSA lowered to 2 m*M*, the morphologies of PANI are shown in Figure 2(a–f). As shown in Figure 2(a), with 1 m*M* SDS, PANI existed as spheres. As shown in Figure 2(b), with 2 m*M* SDS, the morphology of PANI was still spherical. However, as shown in Figure 2(c), with 3 m*M* SDS, a fiberlike morphology of PANI was observed. As shown in Figure 2(d), with 5 m*M* SDS, the fiberlike morphology of PANI still existed but with a much shorter length. As shown in Figure 2(e,f), with 7 or 10 m*M* SDS, PANI showed a spherelike morphology again. For a concentration of DBSA of 30 m*M*, the morphologies of PANI are shown in Figure 3(a–f). As shown in Figure 3(a), with 1 m*M* SDS, PANI existed in a more spherical morphology. As shown in Figure 3(b–e), with 2–7 m*M* SDS, the spherical PANI started to change its shape to cylindrical PANI. The change is shown in Figure 3(e), with 7 m*M* SDS, most apparently. As shown in Figure 3(f), with 10 m*M* SDS, PANI was formed mostly like spheres again. The characteristic

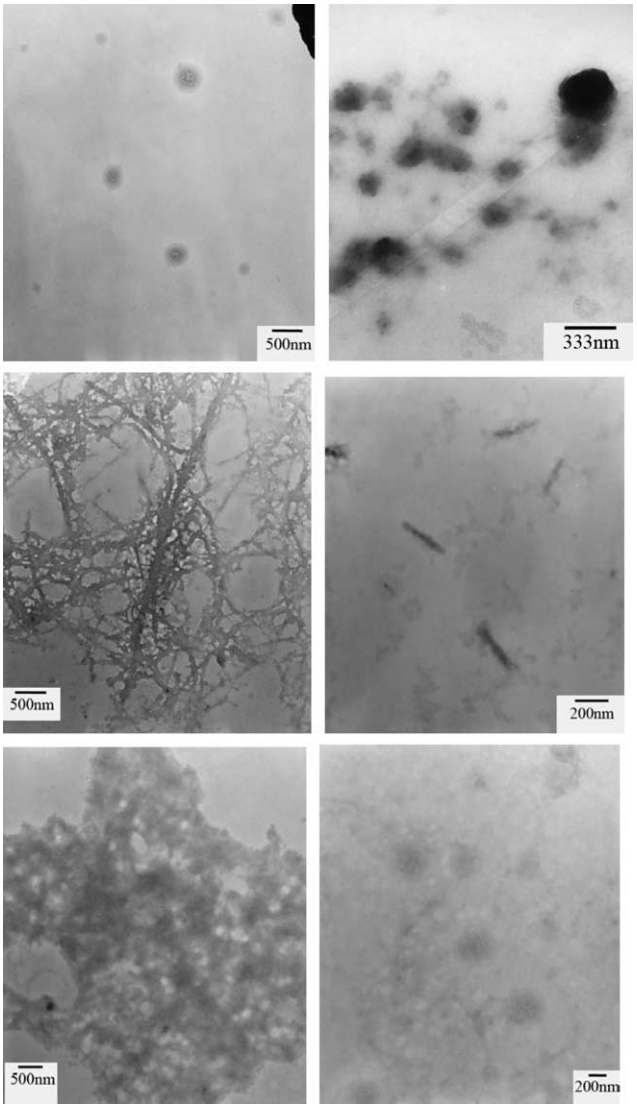


**Figure 2** TEM photographs of PANI with DBSA fixed at 2 m*M* and SDS: (a) 1 m*M* PANID30S01, (b) 2 m*M* PANID30S02, (c) 3 m*M* PANID30S03, (d) 5 m*M* PANID30S05, (e) 7 m*M* PANID30S07, and (f) 10 m*M* PANID30S10.

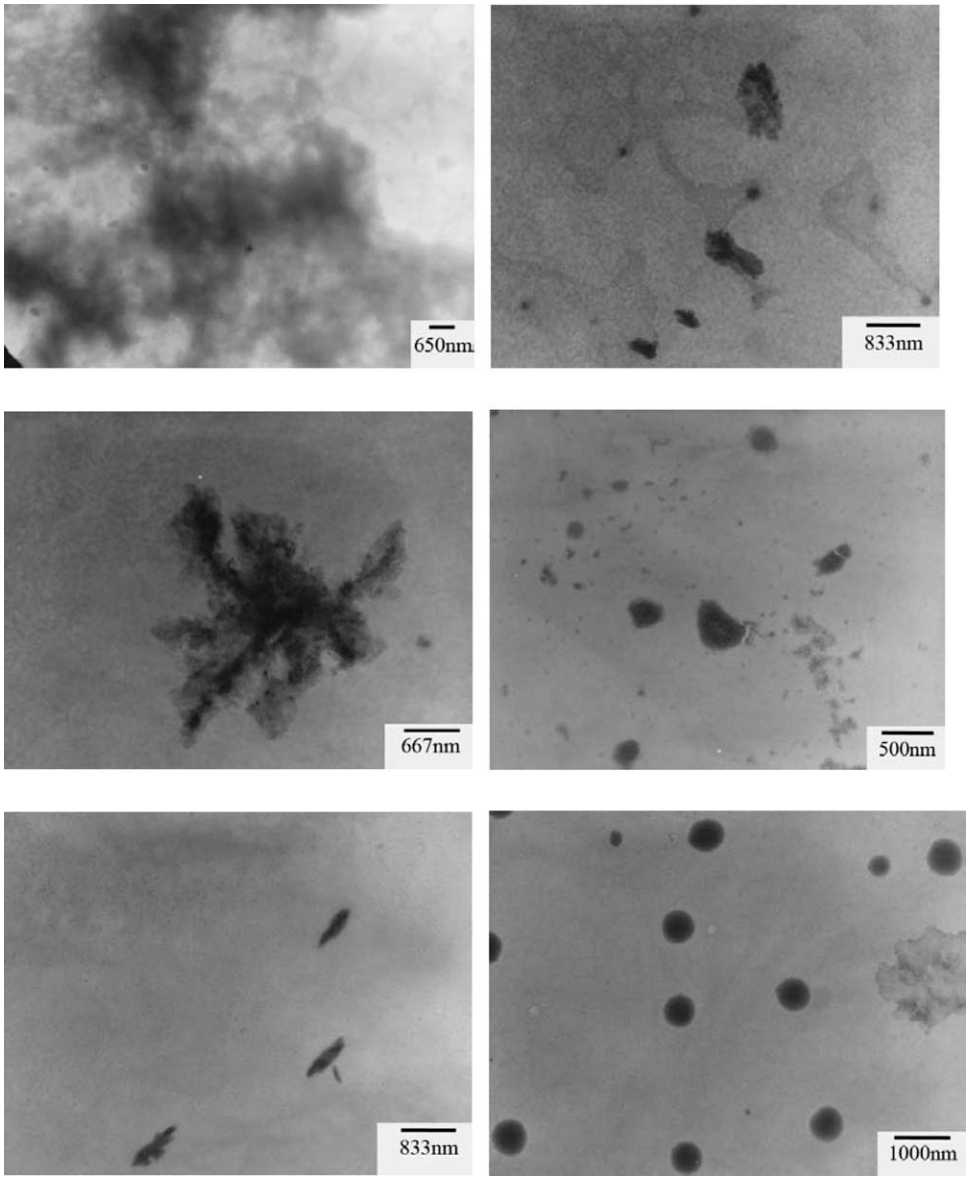


**Figure 3** TEM photographs of PANI with DBSA fixed at 30 m*M* and SDS: (a) 1, (b) 2, (c) 3, (d) 5, (e) 7, and (f) 10 m*M*.

size and shape of PANI shown in the TEM photographs are listed in Table I.

A mechanism was proposed with the scheme in Figure 4 to interpret the morphological changes of the synthesized PANI in a mixture of surfactants as follows.[25] Before SDS was added in the reaction system, DBSA formed micelles itself in the aqueous medium, as shown in Figure 4(a). After the addition of SDS, the incorporation of SDS into the DBSA micelles formed mixed micelles, as shown in Figure 4(b). Both DBSA and SDS molecules rearranged in the mixed micelles, and the mixed micelles were no longer symmetrically spherical in shape.

The measured sizes of DBSA or SDS micelles from the DLS experiments are shown in Figure 5. As shown in Figure 5, both number distribution and volume distribution for each concentration of DBSA or SDS were almost identical; this implied that no large particles were detected by DLS analysis in the systems containing only one kind of surfactant, DBSA or SDS. After the addition of SDS, the measured sizes of the mixed micelles were found to be slightly larger, about 3–4 nm, from the number distribution curves shown in Figure 6, compared with a size of about 0.7 nm of pure DBSA micelles, as shown in Figure 5. It was also found from the volume distribution curves that a small amount of larger particles existed, as shown in Figure 6. This revealed that in the mixture of DBSA and SDS, SDS tended to join the DBSA micelles instead of forming micelles itself.

Furthermore, after the addition of aniline monomer to the DBSA/SDS mixed micelles, very large differences were observed for different concentrations of

**TABLE I**
**Characteristic Size and Shape of the Synthesized PANI**

| Sample | Characteristic size | Shape |
|---|---|---|
| PANI D10S01 | D: 100–250 nm | Spherical |
| PANI D10S02 | D: 70–90 nm<br>L: up to several 10 s μm | Spherical with cylindrical |
| PANI D10S03 | D: 50–70 nm<br>L: up to several 10 s μm | Spherical with cylindrical |
| PANI D10S05 | D: 50–70 nm<br>L: up to several 10 s μm | Spherical with cylindrical |
| PANI D10S07 | D: 70–90 nm<br>L: up to several 10 s μm | Spherical with cylindrical |
| PANI D10S10 | D: 40–50 nm<br>L: up to several 10 s μm | Spherical with cylindrical |
| PANI D30S01 | D: 200–300 nm | Spherical |
| PANI D30S02 | D: 150–200 nm | Spherical |
| PANI D30S03 | D: 50–70 nm | Spherical |
| PANI D30S05 | D: 50–300 nm | Spherical |
| PANI D30S07 | D: 150–200 nm<br>L: 800–900 nm | Spherical with cylindrical |
| PANI D30S10 | D: 200–500 nm | Spherical |
| PANI D02S01 | D: 100–250 nm | Spherical |
| PANI D02S02 | D: 100–300 nm | Spherical |
| PANI D02S03 | D: 30–50 nm<br>L: Up to several 10 s μm | Spherical with cylindrical |
| PANI D02S05 | D: 30–40 nm<br>L: 350–400 nm | Spherical with cylindrical |
| PANI D02S07 | D: 100–500 nm | Spherical |
| PANI D02S10 | D: 100–200 nm | Spherical |

D, diameter of the sphere or spherical end of the cylinder; L, length of the cylinder.

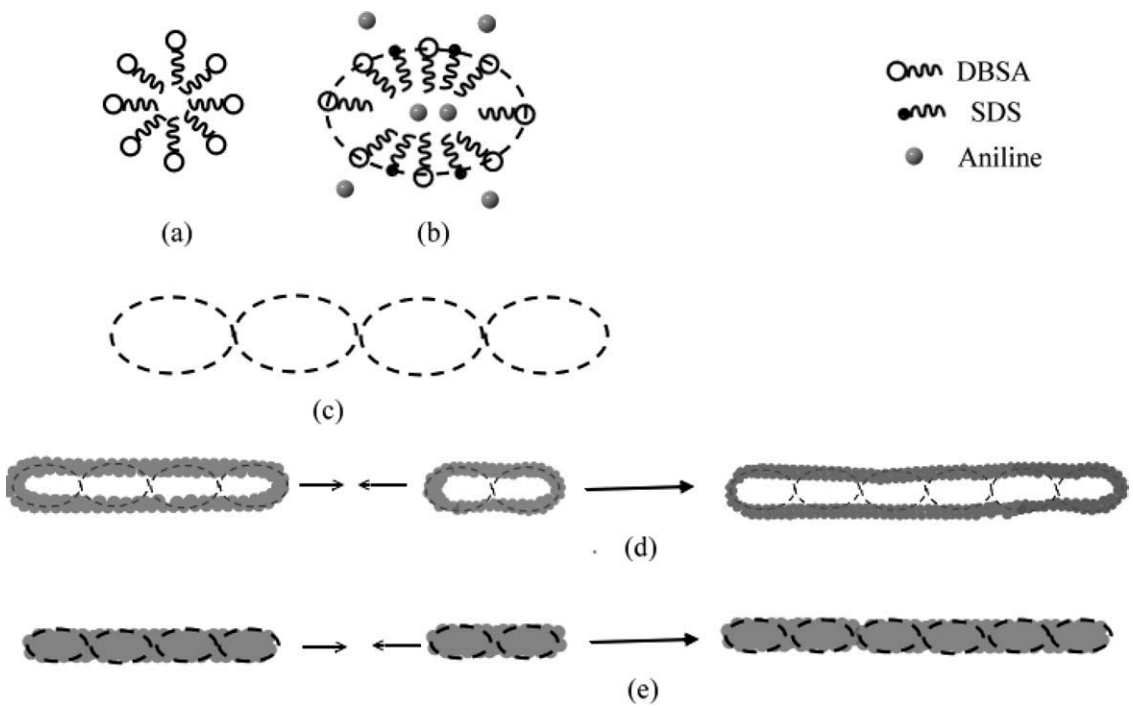


**Figure 4** Schemes of (a) DBSA micelle before the addition of SDS and aniline; (b) micelle of the DBSA, SDS, and aniline mixture; (c) coagulation of the micelles after the addition of aniline monomer; (d) polymerization of aniline at the outside of the micelle to form a tube; and (e) polymerization of aniline at both the outside and inside of the micelles to form fibers.

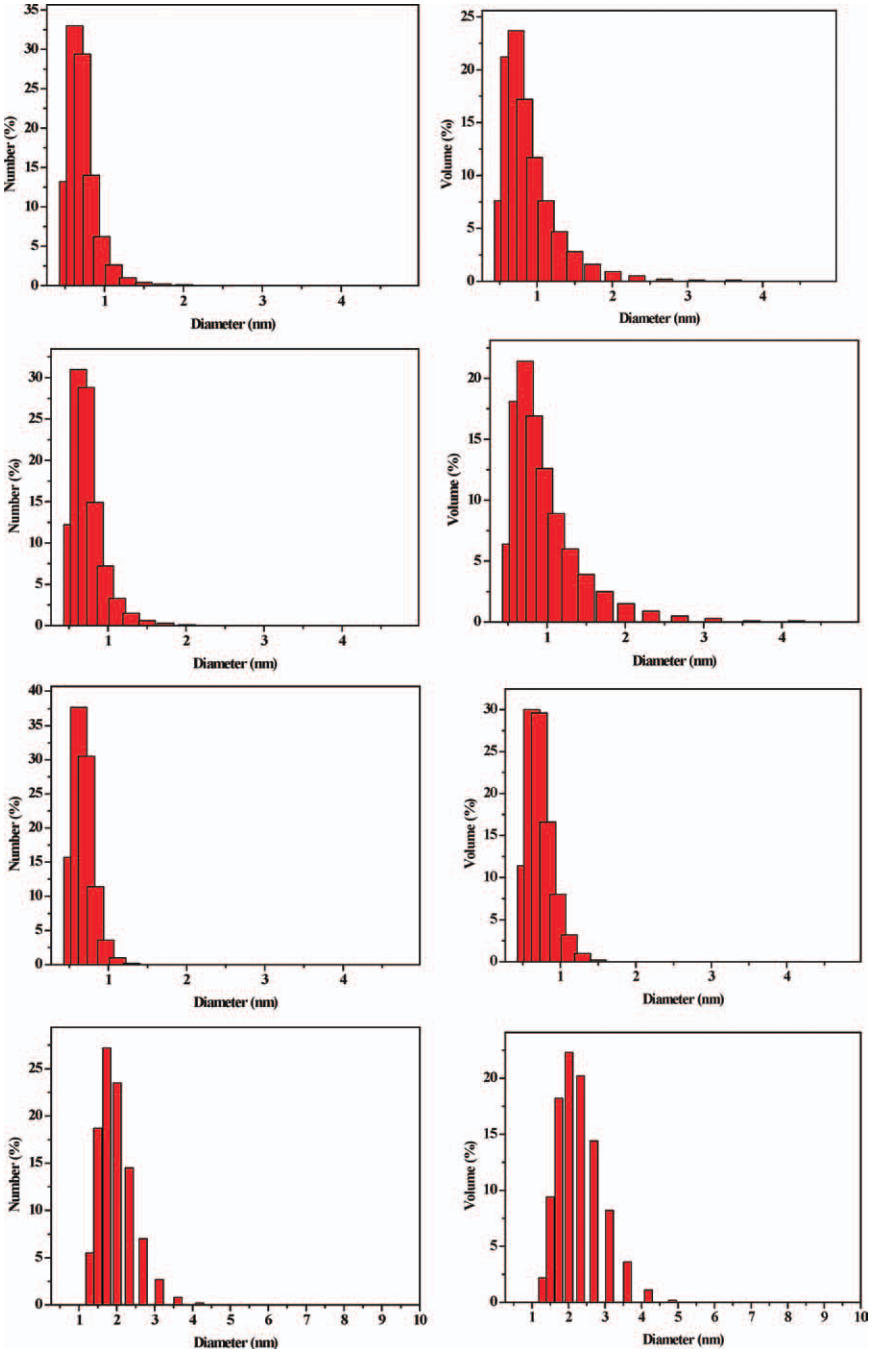


**Figure 5** DLS size analysis of (a) 10 m*M* DBSA, (b) 2 m*M* DBSA, (c) 30 m*M* DBSA, and (d) 10 m*M* SDS. [Color figure can be viewed in the online issue, which is available at wileyonlinelibrary.com.]

DBSA. When the DBSA concentration was 10 m*M*, the addition of 10 m*M* aniline monomer caused the charge density of the mixed micelles to drop significantly and resulted in the coagulation of micelles, as shown in Figure 7(a). The size detected by DLS experiments increased very significantly. When the DBSA concentration was 30 mM, the addition of 10 m*M* aniline monomer lowered the charge density of the mixed micelles, which caused the micelles to shrink, as shown in Figure 7(c). When the DBSA concentration was 2 m*M*, the amount of protons provided by DBSA was insufficient for the protonation of aniline monomers, so that most aniline monomers were hydrophobic and stayed inside the micelles. As shown in Figure 7(b), the size detected by the DLS experiments did not vary much. Consequently, with the addition of aniline monomer, negative charges on the micelles were partially neutralized by positively charged aniline, which provided the mixed micelles more opportunities to coagulate into a cylindrical morphology, as indicated in the scheme of Figure 4(c). During polymerization, cylindrical PANI tended

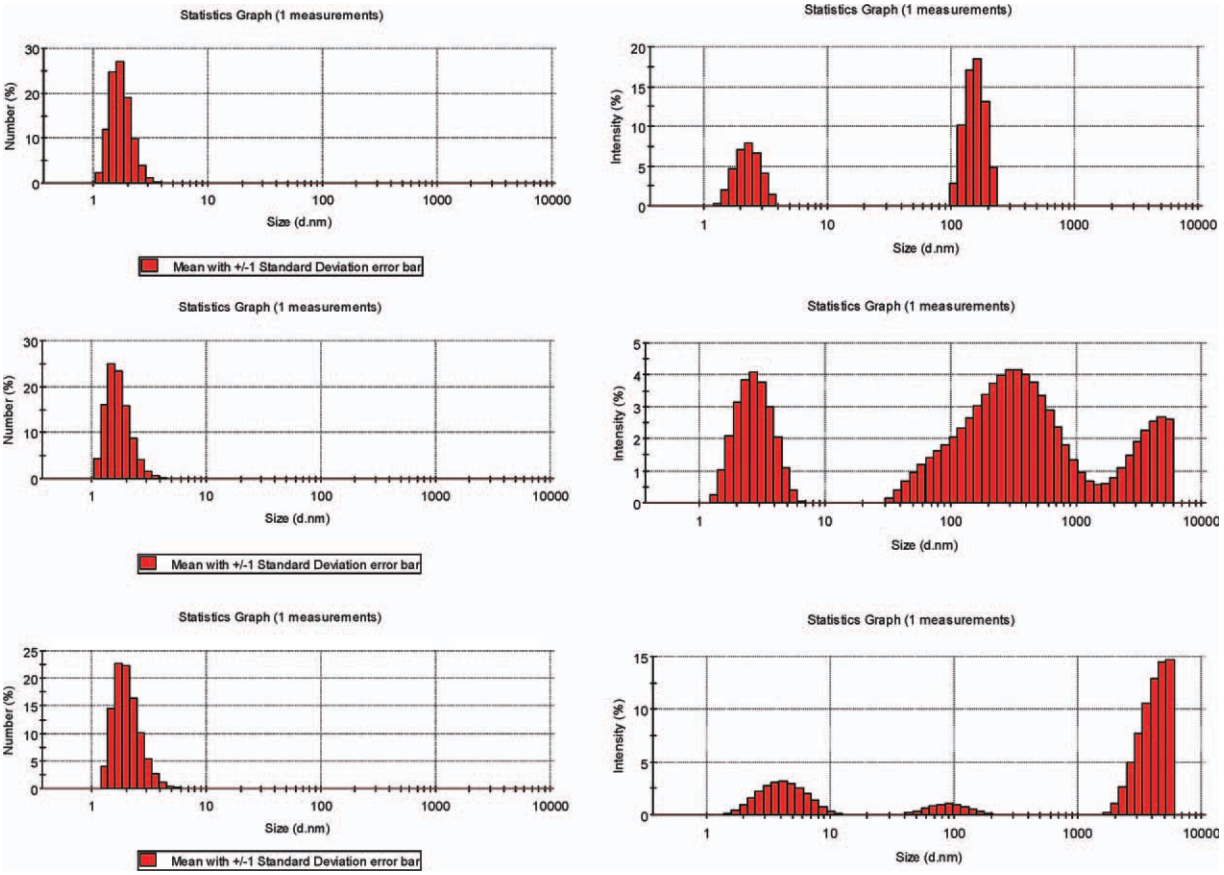


**Figure 6** DLS size analysis of (a) 10 m*M* DBSA and 10 m*M* SDS, (b) 2 m*M* DBSA and 10 m*M* SDS, and (c) 30 m*M* DBSA and 10 m*M* SDS. [Color figure can be viewed in the online issue, which is available at wileyonlinelibrary.com.]

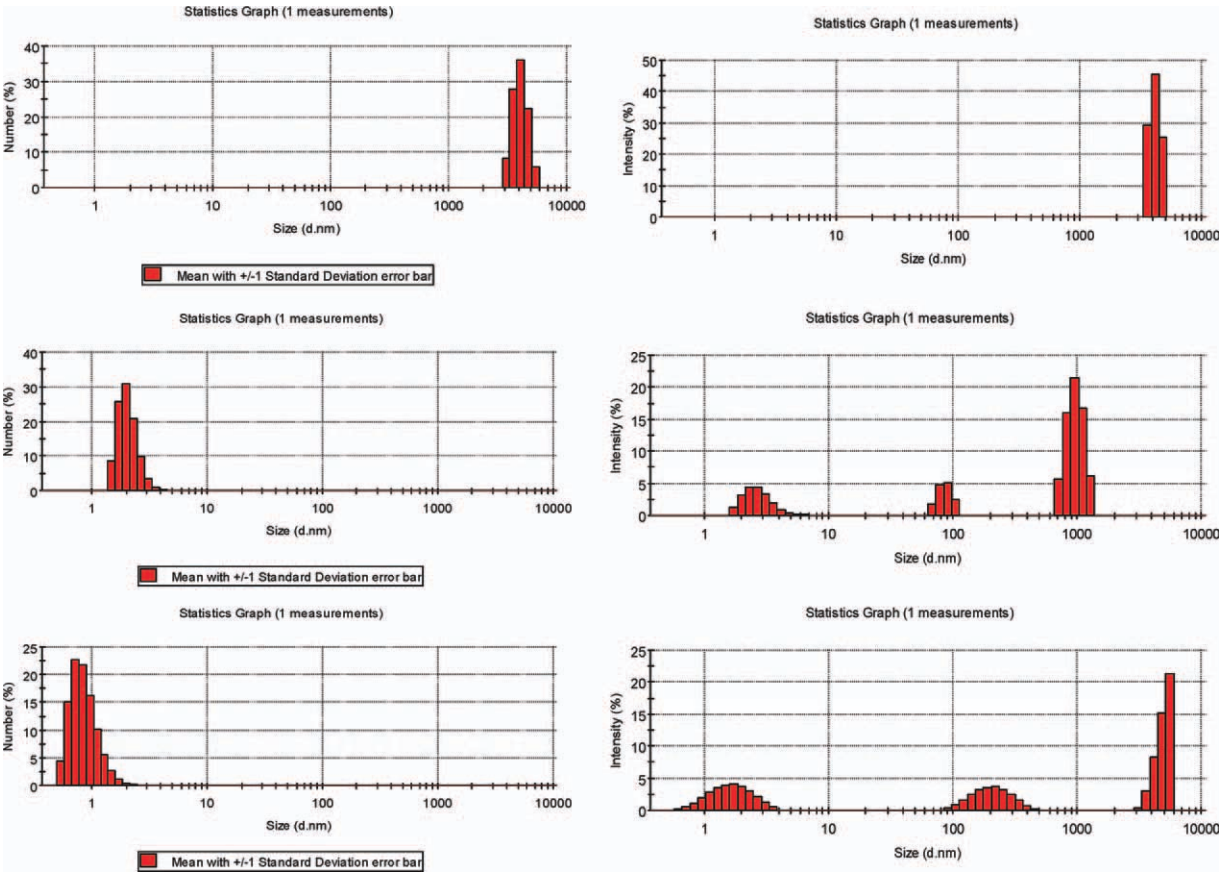


**Figure 7** DLS size analysis of (a) 10 m*M* DBSA and 10 m*M* SDS, (b) 2 m*M* DBSA and 10 m*M* SDS, and (c) 30 m*M* DBSA and 10 m*M* SDS after the addition of 10 m*M* aniline monomer. [Color figure can be viewed in the online issue, which is available at wileyonlinelibrary.com.]

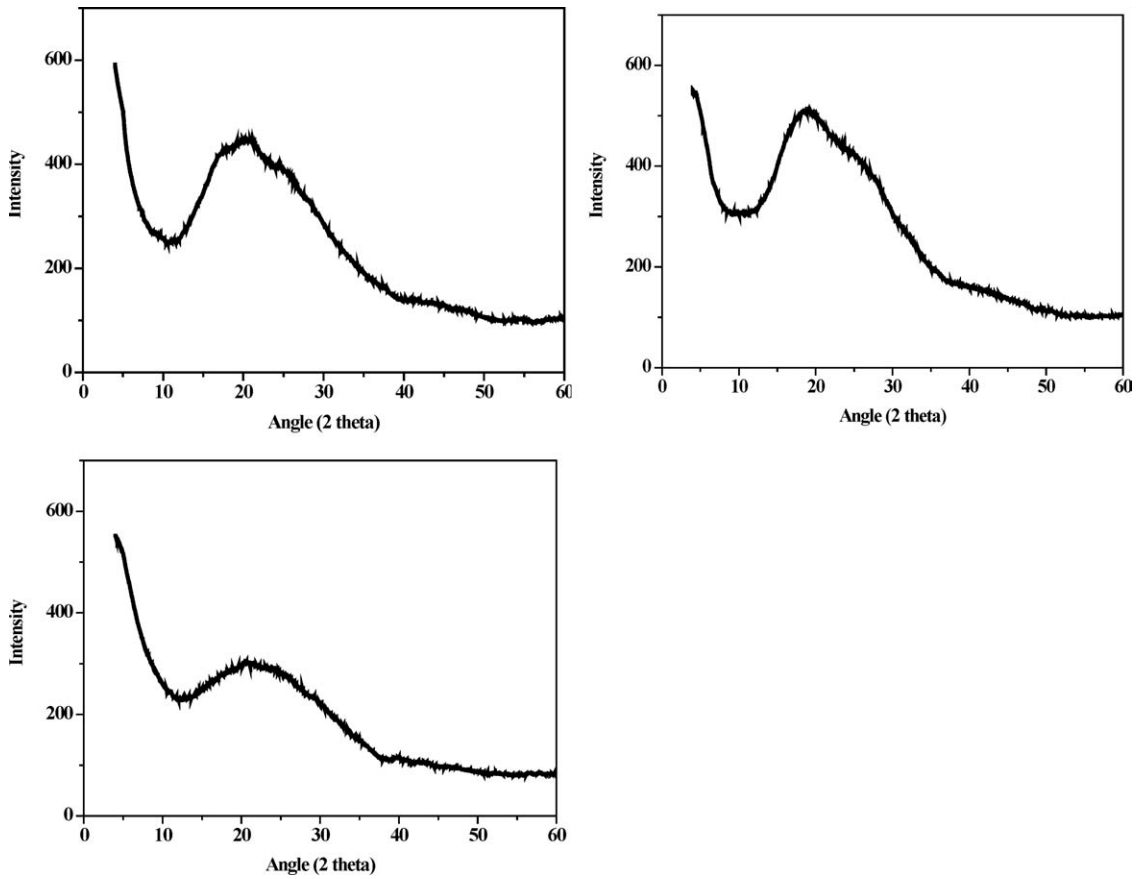


**Figure 8** XRD scans of PANI with 3 m*M* SDS and (a) 10, (b) 2, and (c) 30 m*M* DBSA.

to connect at the ends and elongated with the diameter because the end cap of the cylindrical PANI was relatively unstable because of poor geometric packing and, therefore, had a higher free energy. Such a process elongated the cylindrical PANI, which grew in length as the polymerization proceeded, as shown in Figure 4(d,e). When the concentration of DBSA was 2 or 10 m*M*, the amount of added SDS was relatively comparable to the amount of DBSA. Therefore, it was prone to form mixed micelles and obtain cylindrical PANI, especially in the case of 10 m*M* DBSA. When the concentration of DBSA, as in the case of 30 m*M*, was much higher than SDS, cylindrical PANI was not easily found. In the case of 10 m*M* DBSA, as shown

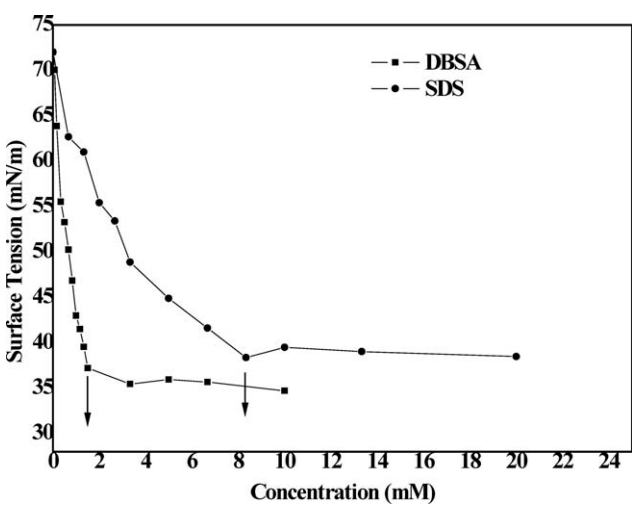


**Figure 9** Surface tension of the DBSA solution and SDS solution.

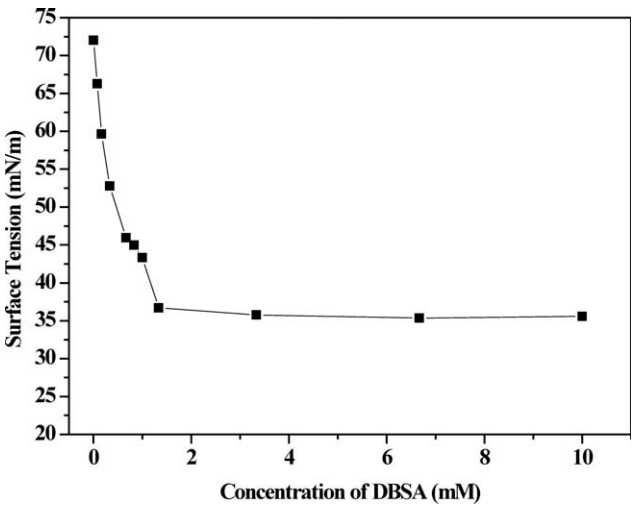


**Figure 10** Surface tension of DBSA with an equal amount of SDS solution.

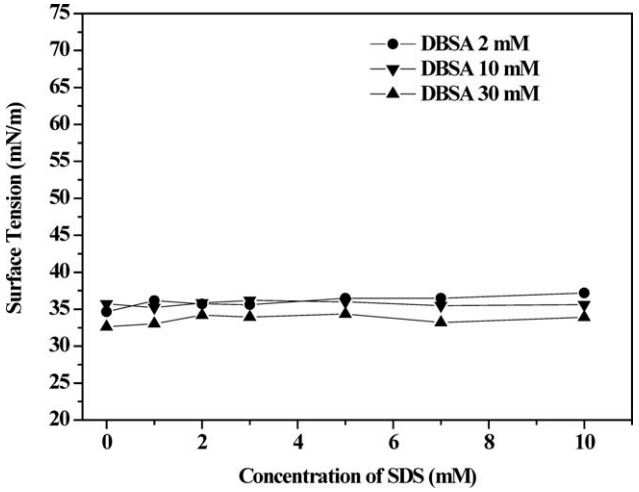


**Figure 11** Surface tension of DBSA solutions with various amounts of SDS.

in Figure 1, some cylindrical PANIs were hollow in structure [Fig. 1(b)], whereas some were solid in structure [Fig. 1(c–f)]. The mechanism proposed by Harada and Adaci[26–27] could be applied to explain our results. Anilinium cations could be solubilized in the micelle–water interface to grow as tubes, or a part of free aniline diffused into the micelles to grow as fibers. When SDS was low in concentration, aniline existed mostly as anilinium cations in the system; thus, PANI grew as tubes. On the other hand, when the concentration of SDS increased, the free aniline increased in amount because of the neutralization of ionic charges; thus, cylindrical PANI showed solid structurelike fibers. XRD scans were also performed in this study, as shown in Figure 8(a–c). For 10 m*M* DBSA, the shoulder at 25° indicated the existence of a peak that represented crystallinity of PANI, and the peak near 20° was reported to be the amorphous peak.[28] For 2 m*M* DBSA, the shoulder at 25° became less clear, and the shoulder was hardly observed for 30 m*M* DBSA. Compared with the TEM photographs, PANI with 10m*M* DBSA showed a more cylindrical morphology, in which the PANI molecules were packed more regularly. Thus, from XRD, we found a more significant peak at 25° for the PANI prepared with 10m*M* DBSA.

The critical micelle concentration (cmc) experiments also supported the purposed mechanism. Figure 9 shows the curves of the surface tension versus the concentration of DBSA and SDS. DBSA had a cmc of 1.8 m*M*, whereas SDS had a cmc of 8.0 m*M*. DBSA decreased the surface tension more effectively. Figure 10 shows the curve of the surface tension versus the DBSA concentration when equal molar concentrations of DBSA and SDS coexisted in the solution. The cmc's of such a system were each 1.7 m*M* for DBSA and SDS. In a comparison of Figures 9 and 10, the concentration of DBSA at critical micelle conditions in the presence of SDS was slightly smaller than that without the presence of SDS. As shown in Figure 11, when DBSA reached the cmc, further addition of SDS seemed to slightly increase the surface tension of the solution. On the other hand, when SDS reached its cmc, as shown in Figure 12, further addition of DBSA slightly decreased the surface tension of the solution. From these experiments, both cmc and the surface tension were affected in the system with the mixed surfactants, DBSA and SDS. This revealed that DBSA and SDS could mutually affect each other in either solution and the micelle structure. For example, in a system with the existence of DBSA micelles, the addition of SDS should tend to replace some DBSA molecules in the micelles to join in and, consequently, change the morphology of the micelles.

The UV–vis spectra of sample latex with 2 mM DBSA were shown in Figure 13. It did not show significant difference for peak shifting of PANI near 800 nm for different concentration of SDS. The peak near 800 nm represents the polaron absorption of the quinoid ring.[29,30]

The FTIR spectra are shown in Figure 14 with 2 m*M* DBSA. In the literature, it was reported that the peak of the emeraldine base protonated with acids is commonly observed at 1162 $cm^{-1}$, the stretching of the benzenoid unit is observed at 1495 $cm^{-1}$, and the stretching of the quinoid unit is observed at 1587 $cm^{-1}$.[31] As shown in Figure 14, the peak of doped PANI shifted to near 1120 $cm^{-1}$ from 1162 $cm^{-1}$. The stretching of the benzenoid unit was shifted to 1489 $cm^{-1}$ from 1495 $cm^{-1}$. The stretching of the quinoid unit was shifted to 1560 $cm^{-1}$ from 1587 $cm^{-1}$. The redshift of the stretching of the quinoid or benzenoid unit implied an increasing degree of charge delocalization on the PANI backbone due to protonation.

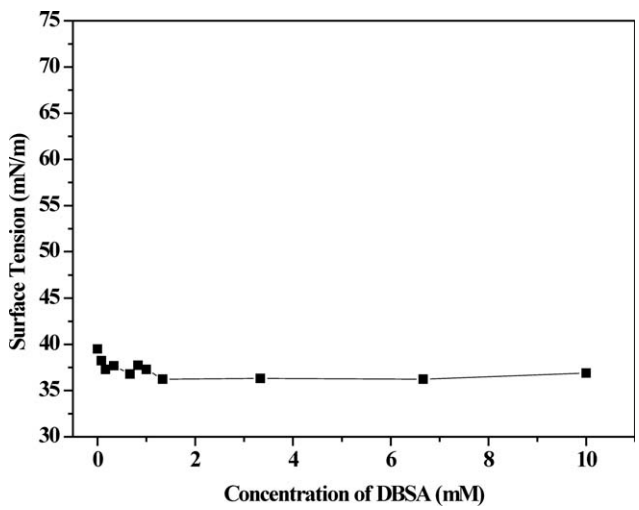


**Figure 12** Surface tension of the DBSA solution with 10 m*M* SDS.

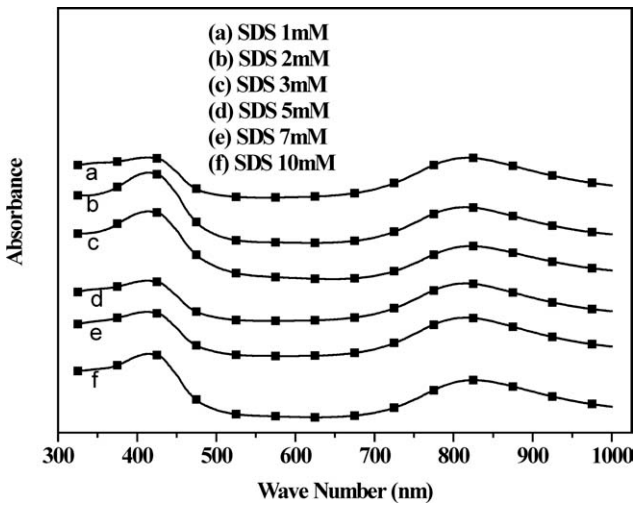


**Figure 13** UV–vis spectra of PANI with 2 m*M* DBSA.

The conductivity of PANI was measured via standard four-probe technology in the form of pellets. A significant increase in the conductivity was observed as SDS was increased from 1 to 3 m*M*, as shown in Table II, when the concentration of DBSA was fixed at 10 m*M*. The improved conductivity was attributed to the morphological change of PANI from spheres to both tubes and fibers; both were cylindrical shape, and the conductivity from fibers was higher than from the tubes. When the concentration of DBSA was reduced to 2 m*M*, poor doping from H+ brought lower conductivities of PANI. Among these samples, only the one, with 3 m*M* SDS, had a little higher conductivity. This was due to the fact that there existed cylindrical PANIs, as shown in Figure 2(c). When the concentration of DBSA increased to 30 m*M*, the conductivities of PANI did not show as much difference as those with 10 m*M* DBSA when we continued to increase SDS. The cylindrical morphology of PANI was least found, compared to the systems of 2 and 10 m*M* DBSA, which led to less improvement in the conductivity.

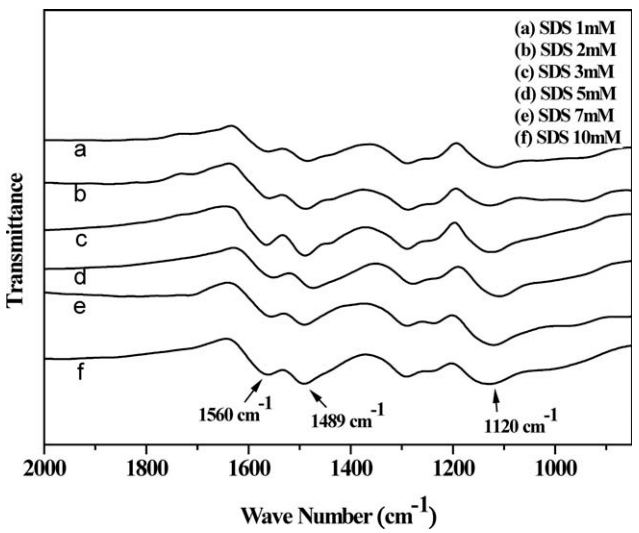


**Figure 14** FTIR spectra of PANI with 2 m*M* DBSA: (a) PANID10S01, (b) PANID10S02, (c) PANID10S03, (d) PANID10S05, (e) PANID10S07, and (f) PANID10S10.

**TABLE II**
**Conductivities of PANI**

| Sample name | DBSA (m*M*) | SDS (m*M*) | Conductivity (S/cm) |
|---|---|---|---|
| PANI D10S01 | 10 | 1 | $5.0 \times 10^{-3}$ |
| PANI D10S02 | 10 | 2 | $2.3 \times 10^{-2}$ |
| PANI D10S03 | 10 | 3 | $2.5 \times 10^{-1}$ |
| PANI D10S05 | 10 | 5 | $2.2 \times 10^{-1}$ |
| PANI D10S07 | 10 | 7 | $2.3 \times 10^{-1}$ |
| PANI D10S10 | 10 | 10 | $2.3 \times 10^{-1}$ |
| PANI D30S01 | 30 | 1 | $6.0 \times 10^{-3}$ |
| PANI D30S02 | 30 | 2 | $5.7 \times 10^{-3}$ |
| PANI D30S03 | 30 | 3 | $7.9 \times 10^{-3}$ |
| PANI D30S05 | 30 | 5 | $8.4 \times 10^{-3}$ |
| PANI D30S07 | 30 | 7 | $1.6 \times 10^{-2}$ |
| PANI D30S10 | 30 | 10 | $1.9 \times 10^{-2}$ |
| PANI D02S01 | 2 | 1 | $8.2 \times 10^{-4}$ |
| PANI D02S02 | 2 | 2 | $8.5 \times 10^{-4}$ |
| PANI D02S03 | 2 | 3 | $1.5 \times 10^{-3}$ |
| PANI D02S05 | 2 | 5 | $9.2 \times 10^{-4}$ |
| PANI D02S07 | 2 | 7 | $8.6 \times 10^{-4}$ |
| PANI D02S10 | 2 | 10 | $9.1 \times 10^{-4}$ |

## CONCLUSIONS

PANI was synthesized in the presence of a mixture of two surfactants, DBSA and SDS. The mutual rearrangement between the two surfactants and the neutralization by positively charged aniline provided the mixed micelles with more opportunities to coagulate into a cylindrical morphology. The cylindrical morphology of PANI was successfully obtained, especially when the amounts of the two surfactants were comparable in the system. For example, in the system of 10 m*M* DBSA, when the SDS concentration was increased from 2 to 10m*M*, a tubular or fiber morphology of PANI was observed. The relative ratio of anilinium cations to free aniline played a key role in whether the tube or fiber morphology was observed. In this work, a significant improvement in the conductivity of PANI was achieved when PANI had a cylindrical morphology.

## References

1. Kim, B. J.; Han, S. G.; Im, S. S. Langmuir 2000, 16, 5841.
2. Kuramoto, N.; Tomita, A. Polymer 1997, 38, 3055.
3. Vincent, B.; Waterson, J. J Chem Soc Chem Commun 1990, 2, 683.
4. Osterholm, J. E.; Cao, Y.; Klavetter, F.; Smith, P. Polymer 1994, 35, 2902.
5. Chen, S. A.; Lee, H. T. Macromolecules 1993, 26, 3254.
6. Yu, L.; Lee, J.; Shin, K. W.; Park, C. E.; Holze, R. J Appl Polym Sci 2002, 88, 1550.

7. Marie, E.; Rothe, R.; Antonietti, M.; Landfester, M. Macromolecules 2003, 36, 3967.
8. Osterholm, J. E.; Cao, Y.; Klavetter, F.; Smith, P. Synth Met 1993, 55, 1034.
9. Osterholm, J. E.; Cao, Y.; Klavetter, F.; Smith, P. Polymer 1994, 35, 2902.
10. Guramoto, N.; Genies, E. M. Synth Met 1995, 68, 191.
11. Kinlen, P. J.; Liu, J.; Ding, Y.; Graham, C. R.; Remsen, E. E. Macromolecules 1998, 31, 1735.
12. Kim, B. J.; Oh, S. G.; Han, M. G.; Im, S. S. Langmuir 2000, 16, 5841.
13. Antonietti, M.; Baten, R.; Lohmann, S. Macromol Chem Phys 1995, 196, 441.
14. Kan, L. M.; Chew, C. H.; Chan, S. O.; Ma, L. Polym Bull 1993, 31, 347.
15. Huijs, F. M.; Vercauteren, F. F.; de Ruiter, B.; Kalicharan, D.; Hadziioannou, G. Synth Met 1999, 102, 1151.
16. Wang, L.-Y.; Lin, Y.-J.; Chiu, W.-Y. Synth Met 2001, 119, 155.
17. Khan, M. A.; Armes, S. P. Adv Mater 2000, 12, 671.
18. Chen, C.-F.; Lee, K.-H.; Chiu, W.-Y. J Appl Polym Sci 2007, 104, 823.
19. Liu, W.; Kumar, J.; Tripathy, S.; Senecal, K. J.; Samuelson, L. J Am Chem Soc 1999, 121, 71.
20. Innis, P. C.; Norris, I. D.; Kane-Maguire, L. A. P.; Wallace, G. G. Macromolecules 1998, 31, 6521.
21. Park, M.; Onishi, K.; Locklin, J.; Caruso, F.; Advincula, R. C. Langmuir 2003, 19, 8550.
22. Kuramoto, N.; Genies, E. M. Synth Met 1995, 68, 191.
23. Kim, B. J.; Oh, S. G.; Han, M. G.; Im, S. S. Synth Met 2001, 122, 297.
24. Li, C.-Y.; Chiu, W.-Y.; Don, T.-M. J Polym Sci Part A: Polym Chem 2007, 45, 3902.
25. Shimizu, T.; Masuda, M.; Minamikawa, H. Chem Rev 2005, 105, 1401.
26. Adachi, M.; Harada, T.; Harada, M. Langmuir 2006, 16, 2376.
27. Harada, M.; Adachi, M. Adv Mater 2000, 12, 839.
28. Chaudhari, H. K.; Kelkar, D. S. J Appl Polym Sci 1996, 62, 15.
29. Wu, F. L.; Wudl, F.; Nowak, M.; Heeger, A. J. J Am Chem Soc 1986, 108, 8311.
30. Stafstrom, S.; Bredas, J. L.; Epstein, A. J.; Woo, H. S.; Tanner, D. B.; Huang, W. S.; MacDiarmid, A. G. Phys Rev Lett 1987, 59, 1464.
31. Drelinkiewicz, A.; Hasik, M.; Choczynski, M. Mater Res Bull 1998, 33, 739.